Molecular dynamics in conducting polyaniline protonated by camphor sulfonic acid as seen by quasielastic neutron scattering

D. Djurado,[1,*] J. Combet,[2,†] M. Bée,[1,2] P. Rannou,[3] B. Dufour,[3] A. Pron,[3] and J. P. Travers[3]
[1]*Université J. Fourier, Grenoble I, Laboratoire de Spectrométrie Physique (UMR 5588-UJF-CNRS), Boîte Postale 87, 38402 St. Martin d'Hères-Cedex, France*
[2]*Institut Laue Langevin, 6 rue Jules Horowitz, Boîte Postale 156, 38042 Grenoble-Cedex, France*
[3]*Laboratoire de Physique des Métaux Synthétiques, UMR 5819 (CEA-UJF-CNRS), DRFMC, CEA, Grenoble 38054, Grenoble-Cedex 9, France*

(Received 18 June 2001; revised manuscript received 3 January 2002; published 9 April 2002)

Using incoherent quasielastic neutron scattering techniques, the molecular motions were investigated in fully hydrogenated and partially deuterated polyaniline protonated by camphor sulfonic acid (CSA) conducting samples. The obtained results show that on the 10^{-9}–10^{-12} s time scale the polymer chains do not exhibit any diffusive motions: the whole observed quasielastic scattering has accordingly to be attributed to motions of CSA ions. From our measurements two molecular movements could be differentiated. A rapid one has been attributed to the three-site rotation of methyl groups present on camphor moieties of CSA and a slower one that has been modeled as a rigid body motion of the whole CSA molecule. Due to the disordered character of the system, the methyl rotors appeared to be dynamically nonequivalent. Their dynamics was then described in terms of a log gaussian distribution of correlation times. This description allowed a good fitting of experimental data and gave an activation energy of 12.5 kJ mol^{-1}. However, two different regimes in temperature could be distinguished. At high temperatures ($T>280$ K) the width of the distribution is nearly zero and thus, the methyl rotors are dynamically equivalent while it turned larger and larger when temperature is decreased below 250 K revealing that the rotors are more and more sensitive to their local environment. In the conducting samples the slowest motion clearly exists in the 280–330 K temperature range and is blocked at temperatures inferior to 250 K. This transition occurs in the temperature range in which the metal-insulator transition also happens.

DOI: 10.1103/PhysRevB.65.184202 PACS number(s): 82.35.Cd, 61.12.Ex, 78.70.Nx

I. INTRODUCTION

Electronic conducting polymers in general and polyaniline in particular have been studied for more than 20 years.[1] Polyaniline (PANI) [see Figs. 1(a) and 1(b)] can indeed be still considered as one of the most promising electronic conducting polymers to be used for practical applications due to both its high chemical and thermal stability in the conducting state.[2] Moreover, since 1992, the discovery of its ability to be relatively easily dissolved when put in the presence of some sulfonated organic protonating acids as camphor sulfonic acid (denominated CSA [Fig. 1(c)] in the following) has increased the scientists' interest even more.[3]

Indeed, this operation sometimes denominated as a ''secondary doping,''[4] allows some highly conducting free-standing films (the electronic conductivity σ typically of the order of several hundreds of S/cm) to be cast from the solvent. Moreover, most of these films exhibit particular transport properties. The electronic conductivity of polyaniline protonated by the camphor sulfonic acid shows a metalliclike behavior typically in a 250–330 K temperature range and then crosses a very broad transition towards an insulating state when temperature is decreased below 250 K.[5] Different groups have developed more or less contradictory contributions in order to give an explanation for such a behavior. The difficulty to find a full agreement partly lies, in our opinion, in the fact that it is still difficult to give a clear picture of the structure and the microstructure of this system. Can PANI/CSA be considered as a 3D homogeneously disordered system or is it a heterogeneous medium mixing fully disordered parts with more organized ones? We recently showed that the answer to these questions strongly depend on which PANI/CSA we are talking about. Indeed, the final structure of solid films are very dependent on the preparation mode and especially the exact characteristics of the starting emeraldine base used in the preparation of the final conducting film.[6] All these experimental difficulties contribute of course to feed even more controversies when analyzing various experimental data from which transport models are tentatively built. A pure 1D model in which the energies required for the creation of electronic excitations as polarons or bipolarons and for their in-chain motion assisted by one or even multiphonon process cannot really account for such high values of the measured conductivity. All the authors are then obliged to take into account some 3D interactions (interchain hopping of electronic excitations) about which most of the controversies are coming from. Some authors developed a model of percolation of metallic bundles in the presence of inhomogeneous disorder and quasi-1D localization,[7] while others are invoking a more ''classical'' 3D Anderson localization model.[8] The possibility of the stabilization of transverse bipolaron via bridging counterion leading to the creation of polaronic clusters in which electronic excitations would be weakly coupled to the lattice, have also been elaborated by other authors.[9–11] In any cases, the coupling of the electronic states with the vibrations of the lattice appears to be a key point to explain the crossover from the metalliclike

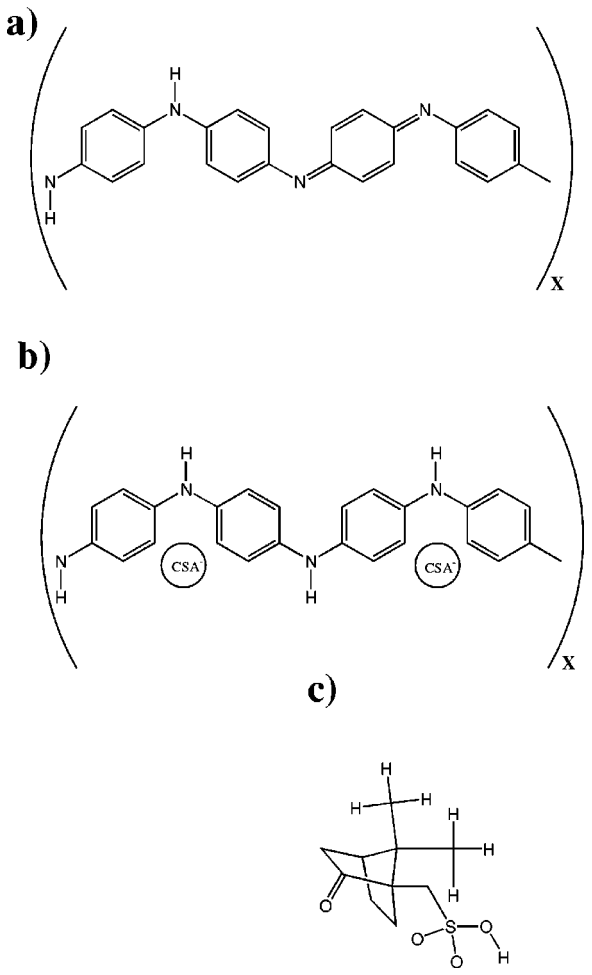

FIG. 1. (a) Emeraldine base (insulating) and (b) Emeraldine salt (conducting) forms of polyaniline. (c) Chemical formula of camphor sulfonic acid.

regime to the insulating one. Particularly, depending on the models, the order of magnitude of transverse transfer integral might be quite different.

The details of the electronic transport in PANI/CSA were extensively studied mainly by using experimental approaches giving access to all the characteristics of the displacement of mobile charge and/or spin carriers (see, for example, most of the references cited in Refs. 7 and 8). In order to study the lattice dynamics, we recently undertook a series of incoherent neutron scattering measurements. Among the large variety of experimental techniques that are available for the investigation of molecular dynamics in organic compounds [nuclear magnetic resonance (NMR), dielectric measurements, . . .] inelastic-and-quasielastic scattering of slow neutrons is certainly one of the most privileged in the sense that it provides both geometrical and frequency (e.g., energy) information about the relevant motions.[12] Furthermore, the use of selectively deuterated samples enables the discrimination between the contributions arising from different parts of the molecules. However, the time scale range accessible to a given spectrometer is usually restricted to one or two orders of magnitude. That does not constitute a severe limitation to the neutron technique but often requires the same specimen to be investigated with several instruments having complementary characteristics in order to get information over a wider energy range. Finally, for highly conducting materials, neutrons also constitute the good probe for looking at the nuclei dynamics without being sensitive to the magnetic spin interaction precisely existing between these nuclei and the conduction electrons. In this paper, we report on a series of quasielastic neutron scattering measurements of the molecular motions in $(C_6H_4)NH^+$-$(CSA)^-_{0.5}$ (abbreviated in the following as PANI-h_5/$(CSA)_{0.5}$ for more simplicity) and $(C_6D_4)NH^+$-$(CSA)^-_{0.5}$ [also called PANI-d_4/$(CSA)_{0.5}$] carried out with several spectrometers on the 10^{-9}–10^{-12} s time scale. In this paper we want to show first that the polymer chains do not exhibit any diffusive motions in the explored time scale and second the dynamics of CSA counterions mainly consists of two components: a rapid one coming from the methyl rotors and a slow one attributed to a rigid body motion of the whole CSA molecule.

The paper is mainly divided in five sections. The first section is devoted to reminding some basic and useful points of the neutron scattering theory. In the second one are described all the experimental conditions concerning the chemical preparation of samples and the neutron scattering measurements. The third section contains all the experimental results tending to prove that in the explored time scale in our experiments, the polymer chains appear as immobile. In the fourth section the dynamics of CSA counterions is fully analyzed while some conclusions are given in the last section.

II. NEUTRON SCATTERING THEORY

A. Expression of the elastic incoherent structure factor

In a typical neutron scattering experiment monochromatic neutrons exchange both energy, $\hbar\omega$ and momentum $\hbar\boldsymbol{Q}$ during the scattering process. The latter is defined as $\boldsymbol{Q}=\boldsymbol{k}-\boldsymbol{k}_0$, where $\boldsymbol{k}$ and $\boldsymbol{k}_0$ are the scattered and incident wave vectors, respectively. As the incoherent scattering length of the hydrogen atoms ($b=25.2\times10^{-15}$ m) is much larger than for deuterium ($b=4.0\times10^{-15}$ m) and an order of magnitude larger than any other scattering length in the system, and as the PANI-h_5/CSA and PANI-d_4/CSA compounds contain a large fraction of hydrogen atoms, only hydrogen incoherent scattering is considered here. Accordingly, when the data obtained with the fully hydrogenated sample will be compared with those of the partially deuterated one, it will be possible to directly evaluate the respective contributions of the polymer chains and the counterions.

The incoherent dynamic structure factor is the time Fourier transform of the intermediate scattering function, $I(\boldsymbol{Q},t)$,

$$S(\boldsymbol{Q},\omega)=\frac{1}{2\pi}\int_{-\infty}^{+\infty} I(\boldsymbol{Q},t)\exp(-i\omega t)dt, \tag{1}$$

where $I(\boldsymbol{Q},t)$ is defined as

$$I(\boldsymbol{Q},t)=\sum_i b_i^2\langle e^{i\boldsymbol{Q}\cdot\boldsymbol{R}_i(t)}e^{-i\boldsymbol{Q}\cdot\boldsymbol{R}_i(0)}\rangle. \tag{2}$$

The sum over i runs over the scattering nuclei in the sample and $\boldsymbol{R}_i(t)$ and $\boldsymbol{R}_i(0)$ denote the vector positions of these nuclei at times t and 0, respectively. The brackets correspond to a thermal average over these positions. The hydrogen atoms of the system experience two types of molecular motions: rotations (reorientations of whole molecule or of chemical groups) and vibrations (phonons and internal vibrations).

The interpretation of the data is usually simplified by making the hypothesis that the different kinds of contributions to motions are essentially not coupled between them, because of their respective time scales and amplitudes. Vibrational motions of a molecule occur on the 10^{-13}–10^{-14} s time scale and may be considered as independent of diffusive-type rotations that are much slower (10^{-9}–10^{-12} s). That is, mathematically expressed by writing the total scattering function as the convolution product of the respective scattering functions

$$S(\boldsymbol{Q},\omega)=S^{\mathrm{rot}}(\boldsymbol{Q},\omega)\otimes S^{\mathrm{vib}}(\boldsymbol{Q},\omega). \tag{3}$$

In the quasielastic region of the spectrum (which corresponds to energy transfers smaller than about 2 meV), the expression above takes the form

$$S(\boldsymbol{Q},\omega)=e^{-\langle u^2\rangle Q^2/3}[S^{\mathrm{rot}}(\boldsymbol{Q},\omega)+S^{\mathrm{inel}}(\boldsymbol{Q},\omega)]. \tag{4}$$

The Debye-Waller term $\exp[-\langle u^2\rangle Q^2/3]$ is a scaling factor that describes the attenuation effect due to lattice phonons or molecule vibrational modes of lowest energy. $\langle u^2\rangle$ stands for the mean square amplitude of vibration. These motions also introduce the inelastic term $S^{\mathrm{inel}}(\boldsymbol{Q},\omega)$ that actually contributes only little to the total scattering in the quasielastic region in the form of a slowly varying function of energy that is most often taken into account as an energy-independent background,

$$S^{\mathrm{inel}}(\boldsymbol{Q},\omega)=S^{\mathrm{inel}}(\boldsymbol{Q}). \tag{5}$$

Correlations between the positions of the same scatterer at initial time $\boldsymbol{R}(0)$ and at a later time $\boldsymbol{R}(t)$ diminish as a function of time and tend to disappear completely at infinite times. Consequently, the thermal average occurring in the intermediate scattering function (2) can be evaluated by considering separately the initial and final positions of the scattering nucleus. Hence, from Eq. (2) and for a single scatterer,

$$I(\boldsymbol{Q},\infty)=\langle e^{i\boldsymbol{Q}\cdot\boldsymbol{R}(\infty)}\rangle\langle e^{-i\boldsymbol{Q}\cdot\boldsymbol{R}(0)}\rangle. \tag{6}$$

The system being in thermal equilibrium, the distribution of the scattering nuclei is the same at both times, so that

$$I(\boldsymbol{Q},\infty)=|\langle e^{i\boldsymbol{Q}\cdot\boldsymbol{R}(\infty)}\rangle|^2=|\langle e^{-\boldsymbol{Q}\cdot\boldsymbol{R}(0)}\rangle|^2. \tag{7}$$

In the case of a fully isotropic sample (liquid), at infinite times, the scattering nucleus can access any coordinate in space, independently of its initial position. Thus the average $I(\boldsymbol{Q},\infty)$ vanishes. Conversely in the case of whole molecule reorientations about center of mass or of internal reorientations of chemical groups, the scatterers remain confined within a certain volume of space. Therefore at infinite times, the probability of finding the scatterer within the volume is equal to unity. $I(\boldsymbol{Q},\infty)$ is directly linked to the Fourier transform of the spatial distribution of the scattering centers so it does not vanish and its variation with the momentum transfer, $\boldsymbol{Q}$, provides information about the size and the shape of the restrictive volume.

At any time, it is possible to separate formally $I(\boldsymbol{Q},t)$ into its time-independent part, $I(\boldsymbol{Q},\infty)$ and its time-dependent part $I(\boldsymbol{Q},t)-I(\boldsymbol{Q},\infty)$. The presence of a constant term gives rise by Fourier transform to a purely elastic component in the scattering function, hence

$$\boldsymbol{S}^{\mathrm{rot}}(\boldsymbol{Q},\omega)=I(\boldsymbol{Q},\infty)\cdot\delta(\omega)+\frac{1}{2\pi}\int_{-\infty}^{\infty}[I(\boldsymbol{Q},t)-I(\boldsymbol{Q},\infty)]\exp(-i\omega t)dt. \tag{8}$$

In the most simple case $I(\boldsymbol{Q},t)$ decreases exponentially with time from its initial value $I(\boldsymbol{Q},0)$ with a single characteristic time τ,

$$I(\boldsymbol{Q},t)=[I(\boldsymbol{Q},0)-I(\boldsymbol{Q},\infty)]\exp\left(-\frac{t}{\tau}\right)+I(\boldsymbol{Q},\infty) \tag{9}$$

and the expression of the scattering function involves a quasielastic component with a Lorentzian shape underlying a purely elastic component. Its half width at half maximum (HWHM), in energy unit is equal to $1/\tau$.

$$\boldsymbol{S}^{\mathrm{rot}}(\boldsymbol{Q},\omega)=I(\boldsymbol{Q},\infty)\cdot\delta(\omega)+[I(\boldsymbol{Q},0)-I(\boldsymbol{Q},\infty)]\frac{1}{\pi}\times\frac{\tau}{1+(\omega\tau)^2}. \tag{10}$$

In the general case of more complicated reorientations or of several scattering atoms having different dynamics, as far as the movements remain diffusive in nature, the quasielastic component is expressed as a sum of several Lorentzian functions whose widths and relative contributions depend on the precise motions of individual atoms.

$$\boldsymbol{S}^{\mathrm{rot}}(\mathbf{Q},\omega)=A(\boldsymbol{Q})\cdot\delta(\omega)+[1-A(\boldsymbol{Q})]\frac{1}{\pi}\sum_i\frac{\tau_i}{1+\omega_i^2\tau_i^2}. \tag{11}$$

In all cases the width of the quasielastic term is directly related to the characteristic times associated with the relevant motions of the scattering nuclei. The overall importance of the purely elastic component $A(\boldsymbol{Q})$ is directly linked to the Fourier transform of the spatial equilibrium distribution of the scattering centers. It has the dimension of a structure factor and is usually denoted as the elastic incoherent structure factor (EISF). Its value can be experimentally obtained considering that

$$A(\boldsymbol{Q})=\frac{I^{\mathrm{elas}}(\boldsymbol{Q})}{I^{\mathrm{elas}}(\boldsymbol{Q})+I^{\mathrm{quasi}}(\boldsymbol{Q})}, \tag{12}$$

where $I^{elas}(\boldsymbol{Q})$ and $I^{quasi}(\boldsymbol{Q})$, respectively stand for the elastic and the quasielastic components of the measured scattering function.

III. EXPERIMENT

In this section, we give some details on the chemical preparation of samples and the experimental techniques. From our point of view, the chemical preparation of samples has to be given here because as mentioned previously in the introductory part, it is of prime importance to specify the exact way the polyaniline samples have been obtained.

A. Chemical preparation of samples

1. Synthesis of hydrogenated PANI

Hydrogenated PANI, hereinafter abbreviated as PANI-*h*, was synthesized by oxidative polymerization of aniline at −25 °C using the method described by Beadle *et al.*[13] It was then converted to hydrogenated emeraldine base (EB-*h*) by treatment with a 0.1*M* aqueous ammonia solution for 72 h and dried under vacuum till obtaining a constant mass.

2. Preparation of films of hydrogenated PANI protonated with CSA-h

Protonation of EB-*h* with CSA was carried out at room temperature using metacresol (MC) as a solvent. The CSA to EB-*h* molar ratio was 0.5. Typically 100 mg of EB-*h* with 127.3 mg of CSA and 19.773 g of MC were mixed together to give 0.5 wt % solution with respect to PANI base. The mixture was vigorously stirred for two weeks at room temperature, then filtered through a 0.20-mm polytetrafluoroethylene PTFE filter. Freestanding films were cast from this solution at 40 °C under room atmosphere. Several batches have been used for the neutron experiments and from elemental analysis results it is quite consistent to consider the mean composition of the sample as $(C_6H_4)NH^+$-$(CSA)^-_{0.5}$ further denoted for more simplicity as PANI-h_5/$(CSA)_{0.5}$.

3. Synthesis of ring-deuterated PANI

Ring deuterated polyaniline was prepared from aniline-d_5 by using chemical oxidation with $(NH_4)_2S_2O_8$. The reaction was carried out at −25 °C.

Reagents. $C_6D_5NH_2$, 7.5*M* DCl solution in D_2O and CH_3OD (all 99 at. % D) were purchased from Euroisotope and used as received. $(NH_4)_2S_2O_8$, LiCl and Na_2CO_3 were dried by extending pumping in vacuum line, prior to use. All other operations were carried out in an atmosphere of dry nitrogen. Typical preparation can be described as follows. First a solution of aniline is prepared in DCl-acidified D_2O/CH_3OD containing LiCl. The exact composition of the solution was 9.8 g (0.1 mol) of aniline, 85 ml of 3*M* DCl in D_2O, 95 ml of CH_3OD and 16 g of LiCl. This solution was mixed with a precooled (−25 °C) oxidizing solution: 6.3 g (0.0275 mol) of ammonium persulfate, 60 ml of 2*M* DCl in D_2O, and 8 g of LiCl. The reaction was carried out with constant monitoring of the temperature and the redox potential. After approximately 2 h a reducing solution consisting of 3.64 g (0.0183 mol) of $FeCl_2$, 5 g LiCl and 50 ml of 2*M* DCl in D_2O was added in order to better control the oxidation state of polyaniline.[13] After an additional 1 h, the reaction was terminated by the separation of the precipitated polymer. The precipitate was then repeatedly washed with DCl/D_2O solution. At this stage the obtained product is polyaniline hydrochloride deuterated both on the ring and the nitrogen atom, i.e., PANI-$d_5(DCl)_{0.5}$. This is caused by the fact that in the reaction mixture deuterium atoms constitute an overwhelming majority (the only existing hydrogen atoms originate from NH_2 group of aniline, -CH_3 group of methanol, and NH_4^+ anion of persulfate). Moreover, the polymer is washed by the solution in which no hydrogen is present (DCl/D_2O). Taking into account quick isotope exchange between PANI amine groups and the doping medium, the resulting polymer must be fully deuterated both on the ring and on nitrogen. Deprotonation of polyaniline deuterochloride with an excess of Na_2CO_3 leads to fully (ring and nitrogen) deuterated PANI base (EB-*d*). Na_2CO_3 being the salt of a strong base and a weak acid gives with D_2O solutions of high *p*H capable of transformation of polyaniline salt into polyaniline base. EB-*d* was then dried under vacuum until reaching a constant mass.

4. Preparation of films of ring-deuterated PANI protonated with CSA

Protonation of EB-*d* with (+/−)-camphor-10-sulfonic acid (H-CSA) was carried out at room temperature using MC as a solvent. The H-CSA to EB-*d* molar ratio was 0.5. Typically 100 mg of EB-*d* with 121.0 mg of H-CSA and 19.779 g of MC were mixed together to give 0.5 wt % solution with respect to PANI base. The mixture was vigorously stirred for two weeks at room temperature, then filtered through a 0.20 mm PTFE filter. Freestanding films were cast from this solution at 40 °C under nitrogen flow.

Doping of EB-*d* with protonic acid in a solvent containing easily exchangeable proton (OH group in *m*-cresol) results in essentially total isotope exchange on PANI nitrogen atoms giving $(C_6D_4)NH^+$-$(CSA)^-_{0.5}$ further denoted PANI-d_4/$(CSA)_{0.5}$ for more simplicity. On the other hand, ring deuterium atoms remain essentially intact because they do not undergo isotope exchange.[14] Thus, deuterated PANI base doped with protonated CSA in protonated MC should exhibit a strong isotopic contrast.

B. The incoherent quasielastic neutron scattering experiments

The IQNS experiments were performed at the high-flux reactor of the Institut Laue-Langevin (ILL, Grenoble, France).

In a first series of experiments, the quasielastic contributions of the PANI-h_5/$(CSA)_{0.5}$ and PANI-d_4/$(CSA)_{0.5}$ systems were measured with the time-focusing time-of-flight spectrometer IN6,[15] with an incident neutron wavelength $\lambda = 5.12$ Å. Spectra were simultaneously recorded at 89 angles, ranging from 14.7° to 113.5°. The experiments were carried out, with the sample set at $\alpha = 135°$ with respect to the incident beam. In such transmission geometry the energy resolution varies from 77 μeV at small scattering angles to

about 120 μeV for the largest values. It was measured with a vanadium plate, 1 mm in thickness, which also served for calibration of the detector's efficiencies. The obtained time-of-flight spectra, after the usual corrections for absorption and scattering from the container were transformed into $S(\theta,\omega)$ using the program INX of the ILL library. A first inspection of the overall intensity of the spectra permitted to identify and to discard the detectors clearly contaminated with Bragg elastic scattering. The remaining data were grouped into a series of 17 spectra spanning the whole scattering angles range. Experiments were performed at temperatures ranging from 101 to 356 K. The temperature stability was about 1 K.

Another series of experiments was performed with the high-resolution backscattering spectrometer IN16,[15] with a wavelength of 6.28 Å and an energy resolution of 0.9 μeV (FWHM). The samples were analyzed also in transmission geometry. Data were recorded at 20 scattering angles, ranging from 10.95° to 135.5° and grouped into five spectra corresponding to average values between $2\theta=21.05°$ and 125.75°. Again, spectra contaminated with elastic Bragg scattering were eliminated from the grouping. The accessible momentum transfer range was similar to IN6 ($Q=0.365$ to 1.78 Å^{-1}). The detector efficiencies were calibrated from the measurement of a vanadium standard and the energy spectra were obtained by using the program SQW of the ILL library. The instrument resolution was determined from the scattering of the sample itself, at $T=3$ K, a temperature at which the scattering is purely elastic. PANI-h_5/(CSA)$_{0.5}$ and PANI-d_4/(CSA)$_{0.5}$ were investigated at eight temperatures ranging from $T=80$ K to $T=330$ K. Deviations in the temperature stability were less than half a degree.

Finally, other measurements have been carried out using the backscattering IN10 spectrometer. This spectrometer is quite similar to IN16 in its principle and exhibits the same resolution in energy (0.9 μeV). The incoming neutron beam had a 6.27 Å wavelength while a $-15/+15$ μeV energy range could be spanned for inelastic scans. As the incoming beam is not focused as it is on IN16, the neutron flux available on the sample is three to four times lower than on IN16.[15] In this study we mainly used IN10 for carrying out fixed energy window measurements when temperature was varied from 3 to 330 K.

IV. RESULTS AND DISCUSSION

A. The different dynamical regimes as evidenced by elastic measurements

A good way to obtain an overall view of the dynamics under interest is to record and inspect carefully the evolution of the elastic intensity as a function of the temperature. Carrying out so-called fixed energy window measurements on backscattering spectrometers like IN16 or IN10 can do that. In such experiments, scattered neutrons are sorted so that only those, which do not exchange energy with the sample (within the energy resolution of the instrument), are detected. To do so using a backscattering spectrometer, it is necessary first to use similar crystals as monochromators and analyzers and second not to sweep in energy by stopping the Doppler

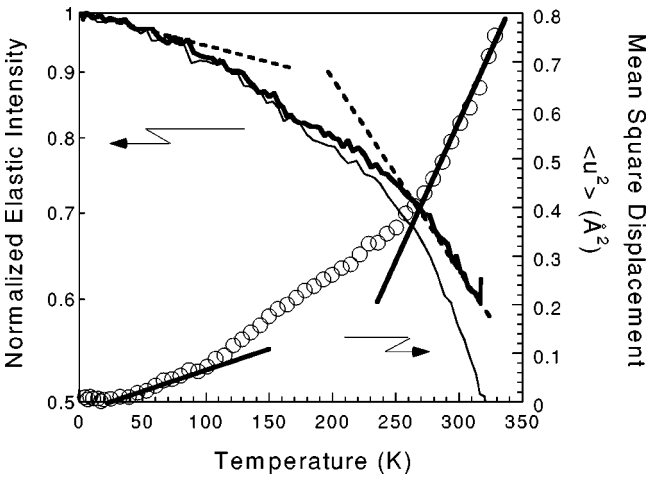

FIG. 2. Evolution of the normalized elastic intensity (displayed on a log scale) measured at $Q=1.24$ Å^{-1} on IN16 as a function of the temperature for PANI-h_5/(CSA)$_{0.5}$ (thick line) and for PANI-d_4/(CSA)$_{0.5}$ (thin line)—broken lines are just guides for the eye. Evolution of the deduced mean square displacement in the same temperature range for PANI-d_4/(CSA)$_{0.5}$. (open circles) straight lines are just guides for the eye.

machine.[16] The occurrence of a molecular motion on the time scale of the spectrometer at a given temperature is inducing a quasielastic broadening of the scattering function and thus a reduction of the detected elastic intensity. Obtained results on IN16 for $Q=1.24$ Å^{-1} with PANI-h_5/(CSA)$_{0.5}$ and PANI-d_4/(CSA)$_{0.5}$ are shown in Fig. 2. Clearly, these curves, whatever way they are drawn, all exhibit two inflection points: one is centered around 100 K and the other around 250 K. Then, it is worth noting that these two inflection points are present on the two curves whatever the PANI chains are deuterated or not. That strongly suggests these two features be only due to motions of protons belonging to CSA counterions. Second, it can be remarked that in amplitude the two normalized curves are quite different. The curve obtained with the fully hydrogenated sample is always above that obtained with the partially deuterated one. In other words, the additional contribution to the total scattered intensity brought by the protons of PANI chains would be mainly if not totally elastic in nature.

In the next paragraph, we present a full analysis of the EISF found both on IN6 and IN16 in order to carefully characterize the chain dynamics as seen in the energy window available in our experiments.

The third curve shown in Fig. 2 is another way to display the experimental data. Indeed, it is always possible to write the dependence of the elastic intensity as a function of the temperature as follows:

$$I(T)=I(0)\exp[-Q^2u(T)^2]. \tag{13}$$

In the previous expression $u(T)$ is the mean square displacement of the scattering nuclei. It is straightforward to obtain the variation of this last quantity as a function of the temperature once that of the elastic intensity has been experimentally measured. By taking into account the large temperature interval separating the two changes of slope, it

appears that the two movements of the counterions thus detected have really different characteristic times. The first motion detected on IN16 at low temperature appears to be quite rapid and the quasielastic broadening is too large to be accurately studied on the IN16 time scale. This is why this motion has been assigned to the methyl groups borne by CSA and has been fully analyzed on the time-of-flight spectrometer IN6 and all the details are given in Sec. IV C 1. Finally, considering the large increase of the mean square displacement around 250 K (Fig. 2), we will see later that this motion appears to be much slower than the other one. It is thus reasonable to assume that this dynamics involves a scatterer with a mass bigger than that of a methyl group. This motion is analyzed in details in Sec. IV C 2.

B. The PANI chains contribution to the dynamics of the system: An EISF analysis

First, it must be said that in all our analyses, we always neglected any eventual contribution coming from metacresol solvent. Indeed, even in the most freshly prepared samples, the latter is in small quantities (never more than 10% molar). Moreover, the solvent content is continuously decreasing as a function of time and also depending on the various thermal treatments undergone by the samples during the different measurements. Accordingly, as it is impossible to evaluate accurately the amount of metacresol in a given film and considering this amount as small enough, we estimated that the error that might be induced in the EISF estimation by ignoring the solvent presence is negligible.

Second, the temperatures at which all the results have been obtained are far below the glass transition of the doped polymer that has been more or less easily evidenced around 400 K.[17,18] In fact, this glass transition is lying close to the temperature of degradation of the system; this is the first indication of the intrinsic semirigidity of PANI chains.

1. TOF measurements (IN6 data—meV energy range)

As previously mentioned, analysis of incoherent quasielastic data mainly consists in the extraction of the experimental values of the EISF from the recorded spectra. In principle, the EISF could be obtained by a simple time-Fourier transformation of the scattering function $S(\boldsymbol{Q},\omega)$. Actually, several conditions rend this procedure rather imprecise. Experimental data are recorded over a limited energy range and are underlain by a flat inelastic contribution $S^{\mathrm{inel}}(\boldsymbol{Q},\omega)$ due to internal and external vibrations. Furthermore, they are obtained at constant scattering angle 2θ and not at constant momentum transfer. Lastly, they have to be corrected for the effects of the finite instrument resolution. Another systematic method has revealed itself to be more successful even in the presence of a weak quasielastic contribution.[19] It consists of a separation of the experimental spectra into their purely elastic and quasielastic parts from a refinement of a ''plausible'' normalized scattering law as close as possible to the actual one, folded with the instrument resolution and where a weight parameter controls the amount of purely elastic scattering. The advantages of this procedure have been described in Ref. 20. In the present case, there is no *a priori* information about the relevant motions. But the fraction of quasielastic scattering in the spectra is small. So a simple scattering law composed of a pure elastic peak and a unique lorentzian function was used.

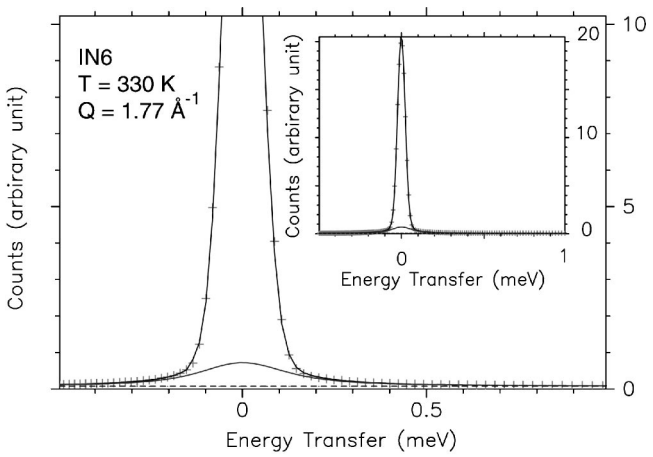

FIG. 3. Expansion of the quasielastic part of a typical energy spectrum measured on the time-of-flight spectrometer IN6, for a momentum transfer $Q=1.77$ Å^{-1}, at $T=330$ K. The full spectrum is shown in the inset. The separation between purely elastic and quasielastic scattering is indicated.

Good fits were obtained for the major part of the refined spectra, confirming that in most cases the quasielastic broadening could effectively be described by a single lorentzian function (Fig. 3). Small discrepancies in the fits were observed at the highest temperatures of the IN6 experiments, for the spectra at the largest Q values. However, careful analysis of these results yielded an estimation of the error on the EISF values of the order of 2%. IN6 values are reported in Figs. 4(a) and 4(b) for PANI-d_4/$(\mathrm{CSA})_{0.5}$ and PANI-h_5/$(\mathrm{CSA})_{0.5}$, at several temperatures. Important features can be noticed by a direct inspection.

The first remark is the dependence of the EISF values on the temperature. Figure 4(a) shows that in the case of the PANI-d_4/$(\mathrm{CSA})_{0.5}$ compound the amount of elastic scattering for a momentum transfer $Q=2$ Å^{-1} increases from 0.82 to 0.93 when the temperature is decreased from 330 to 236 K. A similar behavior is observed with the PANI-h_5/$(\mathrm{CSA})_{0.5}$ system [Fig. 4(b)], with an increase of the EISF from 0.80 to 0.93 over a broader temperature range. Several interpretations concerning this temperature dependence can be put forward and will be discussed later.

The most important point concerns the differences between the EISF values obtained with the two compounds. At any temperature, clearly the values for PANI-h_5/$(\mathrm{CSA})_{0.5}$ lie unexpectedly above the corresponding results for PANI-d_4/$(\mathrm{CSA})_{0.5}$. Moreover, these differences between the two sets of values increase with the temperature. The substitution for the four hydrogen atoms on the benzyl groups reduces the number of ''visible'' scattering centers (i.e., hydrogen atoms) from 25 to 17 and the fraction of scattering from PANI chains from $10/25=0.4$ [PANI-h_5/$(\mathrm{CSA})_{0.5}$] to $2/17=0.118$ [PANI-d_4/$(\mathrm{CSA})_{0.5}$]. Accordingly, the deuteration of benzyl groups should result in an increase of the resulting EISF. The only way to account

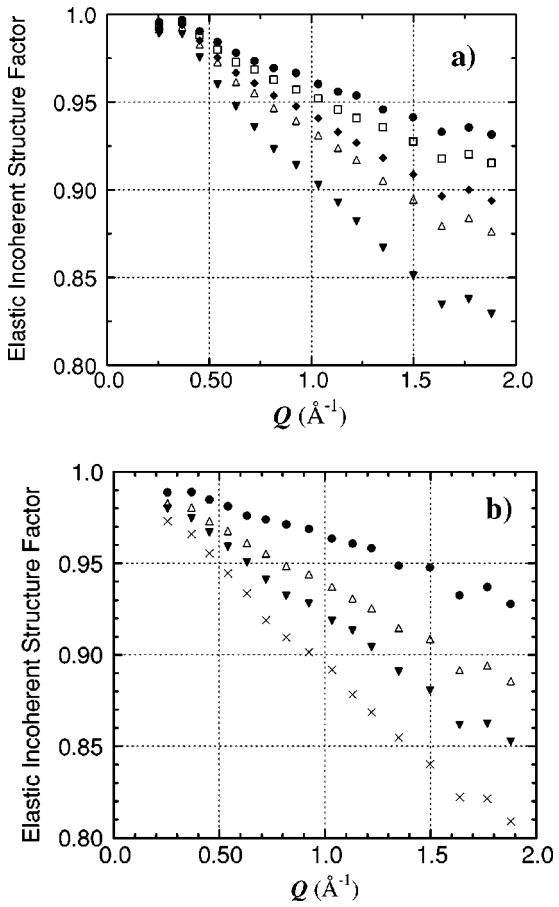

FIG. 4. Experimental values of the elastic incoherent structure factor (EISF) extracted from the IN6 experiments, at different temperatures. (a) PANI-d_4/(CSA)$_{0.5}$, (b) PANI-h_5/(CSA)$_{0.5}$ [(●) 236, (□) 260, (♦) 285, (△) 300, (▼) 330, (×) 356 K]

for the obtained results is to consider that the contribution of benzyl groups is purely elastic, the diffusive motions of the polymer chains being too slow to be seen on our experimental time scale.

2. Backscattering measurements (IN16 data—μeV energy range)

The same remarks hold for the EISF obtained from the IN16 spectra. Good fits were also obtained (Fig. 5). As in the IN6 case, these experimental EISF values depend on the temperature and, at a given temperature differ for the two systems investigated. For PANI-h_5/(CSA)$_{0.5}$, the amount of elastic scattering for a momentum transfer $Q=2$ Å^{-1} increases from 0.72 to 0.9 when the temperature is decreased from 330 to 235 K. With PANI-d_4/(CSA)$_{0.5}$, over the same temperature range, the EISF increases from 0.7 to 0.85.

Thus, once again, for all the temperatures and for all the scattering angles, we found the EISF from PANI-h_5/(CSA)$_{0.5}$ always greater than that of PANI-d_4/(CSA)$_{0.5}$. All the other remarks that can be made about these EISF values found on IN16 compared to that found on IN6 will be made later when we will assign the different dynamics to CSA counterions.

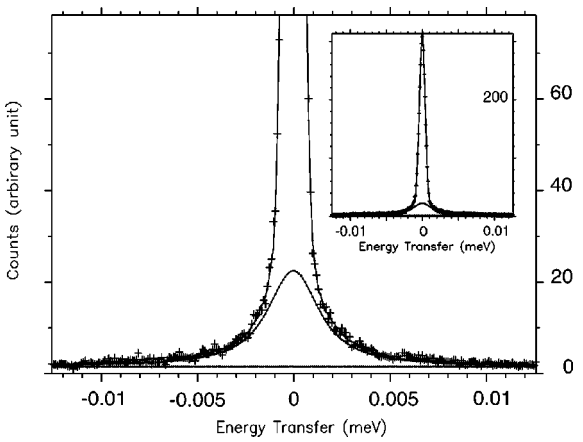

FIG. 5. Expansion of the quasielastic part of a typical energy spectrum measured on the backscattering spectrometer IN16, for a momentum transfer $Q=1.78$ Å^{-1}, at $T=330$ K. The full spectrum is shown in the inset.

As the origin of the difference of the EISF obtained with PANI-h_5/(CSA)$_{0.5}$ and PANI-d_4/(CSA)$_{0.5}$ has to be looked for in the difference of scattering from the hydrogen or deuterium atoms of the benzyl groups in the PANI chain, a quantitative analysis of the experimental EISF values was undertaken.

3. Quantitative analysis of the EISF's

This analysis was performed considering the data obtained with IN16 at $T=300$, $T=330$ K, i.e., with the best instrument resolution at the highest temperatures. The experimental EISF values were refined by an empirical expression of the form

$$\mathrm{EISF}(\boldsymbol{Q}) = a_0 + \sum_{i=1}^{N} a_i \frac{\sin \boldsymbol{Q}\cdot\boldsymbol{R}_i}{\boldsymbol{Q}\cdot\boldsymbol{R}_i} \tag{14a}$$

with

$$a_0 + \sum_{i=1}^{N} a_i = 1. \tag{14b}$$

The expression (14a) is the general expansion of the EISF (Ref. 12) in terms of N jump distances R_i. The parameters are both the R_i and the a_i. Actually it turned out that the expansion could be restricted to $N=3$ terms. At each temperature the data obtained with PANI-h_5/(CSA)$_{0.5}$ and PANI-d_4/(CSA)$_{0.5}$ were refined simultaneously, introducing in the former case, to account for the hydrogenated benzyl groups, an additional fraction of elastic scattering, x, which was also refined, so that the full expression was

$$\mathrm{EISF}(\boldsymbol{Q}) = x + (1-x)a_0 + (1-x)\sum_{i=1}^{N} a_i \frac{\sin \boldsymbol{Q}\cdot\boldsymbol{R}_i}{\boldsymbol{Q}\cdot\boldsymbol{R}_i} \tag{15}$$

with $x=0$ for the PANI-d_4/(CSA)$_{0.5}$ compound.

The results are reported in Fig. 6. The final values of the a_i and R_i parameters are of little interest providing that the procedure attributes the same values to both compounds. The

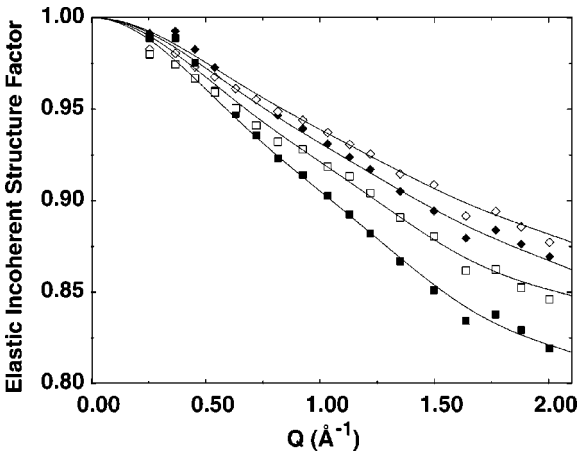

FIG. 6. Experimental values of the elastic incoherent structure factor (EISF) extracted from the IN6 experiments, at $T=300$ K ($\diamond$) and $T=330$ K ($\square$) with PANI-d_4/(CSA)$_{0.5}$ (filled symbols) and PANI-h_5/(CSA)$_{0.5}$ (opened symbols). The full lines are the results of refinements of Eq. (14).

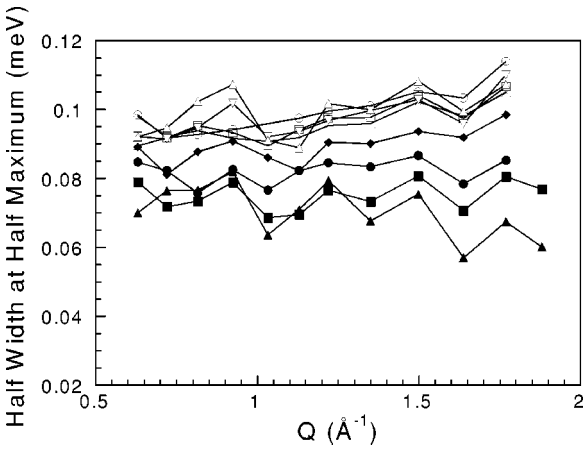

FIG. 7. Half width at half maximum of the quasielastic part of scattering profiles obtained in transmission geometry on IN6 as a function of the transfer momentum Q and the temperature. (Opened symbols refer to PANI-d_4/(CSA)$_{0.5}$ and filled symbols to PANI-h_5/(CSA)$_{0.5}$) ($\blacklozenge$) 356, ($\bigcirc$) 330, ($\square$) 300, ($\times$) 285, ($\triangledown$) 260, ($\triangle$) 235 K.

main result concerns the parameter x, which was found equal to 0.35 at each temperature, close to the theoretical value $x=0.32$ corresponding to immobile benzyl groups.

This result definitively demonstrates that within the $10^{-9}-10^{-12}$ s time scale, the PANI chains can be considered as immobile while the observed localized motions are exclusively due to CSA molecules.

C. Analysis of the CSA counterions dynamics

1. Analysis of the motion of CSA methyl groups in conducting PANI/CSA from TOF measurements

Generally speaking, methyl groups dynamics is extensively studied in many different solid-state systems because it may be considered as a microscopic probe able to reveal the details of the neighboring local molecular and energetic environments. In particular, methyl groups dynamics has been investigated in systems including small molecules[21] and polymeric compounds.[22–24] In many cases, this motion can be described as jumps on three energetically equivalent sites evenly distributed on a circle.

Accordingly, we started by analyzing our data using this description. The theoretical scattering law for 120° jumps of a CH_3 group can be written (powder average) as[12]

$$S_{\mathrm{meth}}(\boldsymbol{Q},\omega)=A_0(\boldsymbol{Q})\,\delta(\omega)+[1-A_0(\boldsymbol{Q})]\,\frac{1}{\pi}\,\frac{\Gamma}{\Gamma^2+\omega^2} \tag{16}$$

with

$$A_0(\boldsymbol{Q})=\tfrac{1}{3}[1+2j_0(\sqrt{3}\boldsymbol{Q}\cdot\mathbf{r})]. \tag{17}$$

In expressions (16) and (17), r is the distance of the hydrogen atom to the threefold symmetry axis, Γ is the jumping rate (which defines the HWHM of the quasielastic component) which is related to the correlation time—mean residence time between two consecutive jumps—by $\Gamma=3/2\tau$.

Only methyl groups are assumed to be dynamically disordered on the considered time scale. The movements of other atoms are expected to be out of the spectrometer resolution. Accordingly, their contribution to the scattering law is purely elastic and appears in the model as a constant parameter c_{fix}. This quantity only depends on the chemical composition of the samples and takes the value 0.647 for PANI-d_4/(CSA)$_{0.5}$ and 0.76 for PANI-h_5/(CSA)$_{0.5}$. Spectra were then refined using the program AGATHE (Ref. 25) and compared with the final theoretical model

$$S_{\mathrm{inc}}^{\mathrm{reo}}(\boldsymbol{Q},\omega)=e^{-W(Q)}\{(1-c_{\mathrm{fix}})S_{\mathrm{meth}}(\boldsymbol{Q},\omega)+c_{\mathrm{fix}}\delta(\omega)\}. \tag{18}$$

By using the previously described scattering law, time-of-flight spectra were first refined individually at 357, 330, 300, 230, and 180 K. Within the experimental errors, the extracted widths appeared as constant over the whole Q range (Fig. 7). This is consistent with the 120° jump model for which the quasielastic contribution is indeed independent of the scattering angle. But, this model apparently does not hold any more when the noticeable variation of the extracted EISF as a function of the temperature is taken in consideration (see Fig. 4). Finally, contrarily to what is usually observed with such a model, the evolution of the characteristic time does not follow an Arrhenius law and asymptotically tends to a common value when the temperature is decreased.

At this stage, it should be noted that similar features were observed in some molecular crystals or in the glassy state of amorphous polymers containing methyl groups. The only way to account for all these experimental observations is to consider that all the methyl groups are not dynamically equivalent. In such a case, several descriptions of the system are possible and have been used alternatively by different authors. The simplest one is to consider a bimodal distribution of methyl groups: one part has a fast enough dynamics and can be observed on the time scale of the instrument, whereas the other part is considered as immobile. The evo-

lution with the temperature results in a modification of the ratio between the two respective populations. A more sophisticated description has been recently proposed by Frick and Fetters[22] in order to explain the temperature dependence of elastic window measurements on polyisoprene. A Gaussian-like distribution of activation energy was introduced and allowed elastic scans to be fitted properly. The same procedure was used by Arrighi *et al.* when studying methyl groups in liquid crystalline polymers.[23] In the present work, we decided to follow the procedure recently developed by Chahid, Alegria, and Colmenero[26] for the study of poly(methyl methacrylate) and used also by Arrighi and Higgins for studying a liquid-crystalline polyester.[27] The distribution of the correlation times has now a log-Gaussian expression and is inserted in the so-called ''rotation rate distribution model.'' In that case, each methyl group motion is assumed to follow an Arrhenius law as

$$\Gamma(T)=\Gamma_{\infty}\cdot\exp(-E_{\mathrm{act}}/kT) \tag{19}$$

with Γ_{∞} and E_{act} being the attempt frequency and the activation energy, respectively. Then, the global distribution of correlation times may be the resultant of a distribution of either the activation energy or the attempt frequency or a combination of both.

For the calculation it is more convenient to use a discrete form of the distribution[28] and the scattering law is written as

$$S_{\mathrm{inc}}^{\mathrm{reo}}(\boldsymbol{Q},\omega)=e^{-Q^2\langle u^2\rangle/3}\Big\{(1-c_{\mathrm{fix}})\Big(A_0(\boldsymbol{Q})\,\delta(\omega)+(1-A_0)\sum_i g_i L_i(\boldsymbol{Q},\omega)\Big)+c_{\mathrm{fix}}\delta(\omega)\Big\} \tag{20}$$

with $\Sigma g_i=1$ and

$$g_i\propto g(\ln\Gamma_i)=\frac{1}{\sigma\sqrt{2\pi}}\exp\left[-\frac{1}{2\sigma^2}\ln^2\left(\frac{\Gamma_i}{\Gamma_0}\right)\right]. \tag{21}$$

In the expression (20) Γ_0 denotes the most probable jump rate and σ^2 is the variance of the distribution. To each Lorentzian function L_i corresponds a HWHM Γ_i and a weight g_i. Spectra recorded at the different angles were first refined individually at each temperature. The distribution function was limited in the $\pm 6\,\sigma$ interval. Twenty Lorentzian functions were used for the evaluation of the scattering function. The EISF was kept fixed at its theoretical value and was not refined. As Bragg scattering is mostly present at low scattering angles,[29] this angular region was not included in the refinement procedure.

Obtained values of Γ_0 and σ are shown in Figs. 8(a) and 8(b) at various selected angles and temperatures. At each temperature, all these values appear to be distributed around a single average one within the experimental error. Finally, we carried out the simultaneous refinement at every angle and we found very similar results for Γ_0 and σ. All the final values are collected in Table I. In Fig. 9 are shown the obtained profiles of the distribution plotted as a function of E/kT overlaid with the energy windows that can be explored

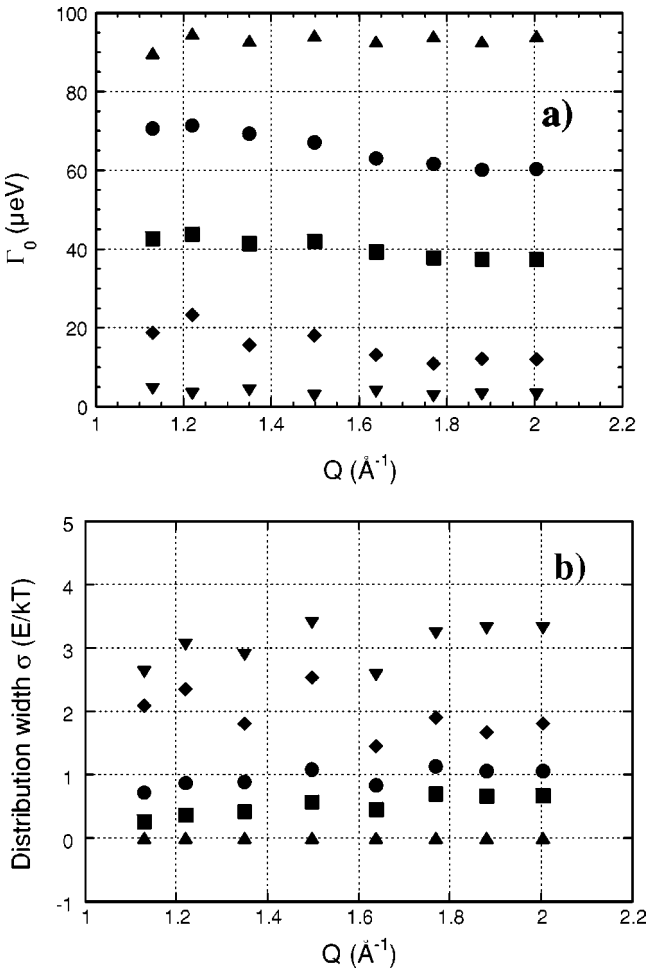

FIG. 8. (a) Most probable jumping rate Γ_0 as a function of the scattering vector and of the temperature deduced for PANI-h_5/(CSA)$_{0.5}$. (b) Width of the correlation time distribution σ as a function of the scattering vector and of the temperature deduced for PANI-h_5/(CSA)$_{0.5}$. (▲) 357, (●) 330, (■) 300, (♦) 235, (▼) 185 K.

by the different spectrometers we used. This figure illustrates well in which proportion the population of scattering centers is varying as a function of the temperature; accordingly, it becomes clear why the apparent EISF deduced from measurements recorded on a given spectrometer was also accordingly varying.

In Fig. 10 is shown first, the Arrhenius plot of the variation of Γ_0 as a function of temperature. From this curve, and from expression (19), it is found that $\Gamma_{\infty}=7.84$ meV and $E_{\mathrm{act}}=12.5$ kJ/mole. This last value corresponds to typical values encountered in the literature concerning other molecular systems containing methyl rotors and in particular to the NMR results obtained with pure camphor.[30] By contrast this value is much larger than that found in the case of the glassy state of polymers having methyl rotors bounded to the main chain.[28] That underlines the difference of nature of considered systems and also of the exact character of molecular disorder. Even if the disordered character of PANI-CSA is extended enough to compel us to use a description of the methyl dynamics with a distribution of correlation times, the

TABLE I. Characteristics of the CSA methyl groups dynamics: Correlation times and their distribution.

Temperature (K)	Most probable jumping rate Γ_0 (μeV)	Reorientation time τ (10^{-12} s)	Width of the distribution σ	Variance of the distribution σ^2
357	93.2	6.97	0.008	6.4×10^{-5}
330	75.4	8.61	0.897	0.805
300	55.5	11.7	1.622	2.631
284	51.0	12.7	2.240	5.018
265	24.9	26.1	2.790	7.784
235	14.1	46.1	3.565	12.71
185	2.0	325.0	4.400	13.80

activation energy we found reveal that the local environment of the methyl rotor is not fundamentally different from the one encountered in a molecular crystal. In other words, the short-scale molecular landscape is probably less entangled than it might be in a glassy state of a flexible polymer.

Considering now Table I and the second curve of Fig. 10 it can be seen that the best description of the variation of the width of the distribution σ as a function of the temperature is a linear one whose numerical parameters are given in the expression

$$\sigma = 0.0261 \times (364 - T). \tag{22}$$

Once again this behavior contrasts with that found in the case of methyl dynamics in glassy states of polymers. In the present case, the width of the distribution is zero for a finite value of the temperature. Accordingly, for PANI-CSA, it cannot be said that the origin of the distribution of the correlation times is exclusively due to a temperature-independent Gaussian distribution of activation energy as it has been found in the case of the glassy state of Poly(vinyl acetate).[28] In PANI-CSA, the heterogeneous character of the structural disorder of the sample has probably to be taken into account. The distribution of correlation times is likely due for a given part to deviations of equilibrium positions of nuclei but also it is necessary to consider several types of populations of methyl groups according to the more or less crystallized domains of the sample they belong to. Moreover, considering in more details the numerical values of σ, it can be seen that for temperatures higher than 280 K, σ is inferior to 1 and even very close to zero at 357 K. In this regime, the methyl group's dynamics is not affected by the intermolecular effects. By contrast for lower temperatures, σ is increasing rapidly revealing a strong influence of the molecular environment on the dynamics of the methyl groups.

In order to check the self-consistency of the previous analysis, we can use all the parameters and expressions found from measurements and from the different fitting procedures in order to recalculate the value of the elastic inten-

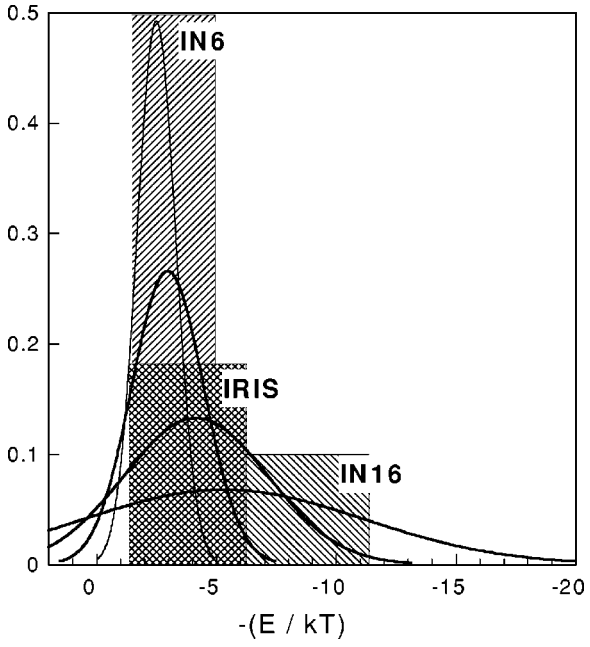

FIG. 9. Shape and position of the distribution of the correlation times as a function of the temperature. The energy windows explored by the different spectrometers used in this work are also indicated.

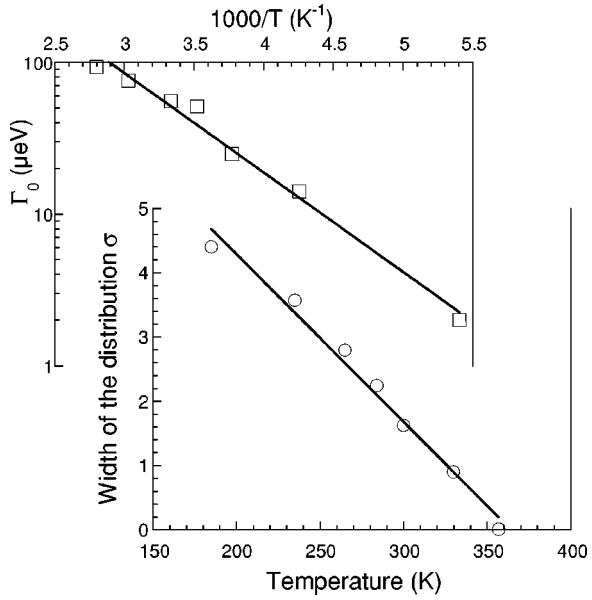

FIG. 10. Most probable jumping rate Γ_0 as a function of the temperature. (The straight line corresponds to the exponential fit according to expression (19) with $\Gamma_\infty = 7.84$ meV and $E_{act} = 12.5$ kJ/mole). Variation of the width of the distribution of correlation times as a function of the temperature. The straight line corresponds to the linear fit according to expression (22).

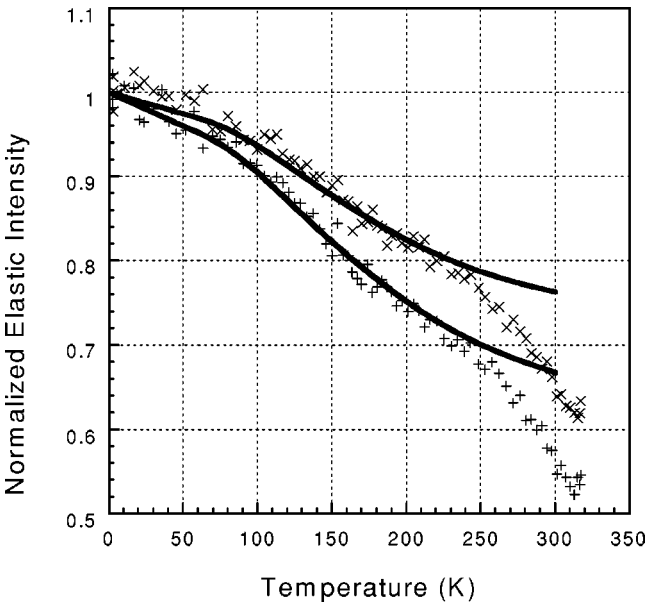

FIG. 11. Elastic intensity measured on IN16 at $Q=1.24$ Å^{-1} ($\times$) and $Q=1.56$ Å^{-1} ($+$) as a function of the temperature for PANI-h_5/(CSA)$_{0.5}$. The full lines are the results of simulations using the parameters obtained from measurements and analysis carried out with IN6 spectrometer in the 200–350 K temperature range, i.e., $E_{act}=12.5$ kJ/mole $\Gamma_\infty=7.84$ meV, $u^2=0.0005\times T$ (Å^2) (mean square displacement), $\sigma=(364-T)\times 0.0261$, fixed protons$=0.76$.

sity as a function of the temperature but extrapolated to the energy domain seen by backscattering spectrometers such as IN10 and IN16. Selected results of this calculation are shown in Fig. 11 for $Q=1.24$ and 1.56 Å^{-1}. By this way, we check first that indeed the first change in these curves was due to the methyl groups dynamics and second was due to the fact that the undertaken analysis is self-consistent. It should be also noted that other measurements we carried out on IRIS spectrometer at ISIS (Chilton-GB) unambiguously proved that the previous connection between IN6 to IN16 we are making by interpolation is correct since the methyl rotor motion could be followed on IRIS over the whole intermediate energy range.[31]

2. Analysis of the rigid body motion of CSA molecules in conducting PANI/CSA from neutron backscattering measurements

As shown in Fig. 12, it is noteworthy that the experimental EISF values obtained with IN16 are smaller than those extracted from the IN6 data, at the same temperature (0.72 and 0.82 at $Q=2$ Å^{-1} with IN16 and IN6, respectively, for PANI-d_4/(CSA)$_{0.5}$ at $T=330$ K). Moreover, the deviations between the two sets of values corresponding to the hydrogenated or deuterated systems are more marked with IN16 than with IN6. The difference is only 3% at $Q=2$ Å^{-1}, $T=330$ K for IN6 while it reaches 13% with IN16 under the same experimental conditions. Actually, taking into account the large difference between the energy resolutions of the two spectrometers, it is unlikely that the same microscopic motion could be observed. Figure 5 illustrates the result of

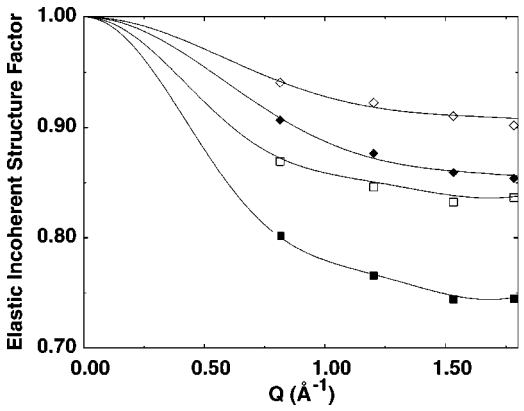

FIG. 12. Experimental values of the elastic incoherent structure factor (EISF) extracted from the IN16 experiments, at $T=300$ K ($\diamond$) and $T=330$ K ($\square$) for PANI-d_4/(CSA)$_{0.5}$ (filled symbols) and PANI-h_5/(CSA)$_{0.5}$ (opened symbols). The full lines are the results of refinements using Eq. (24).

the refinement of the PANI-d_4/(CSA)$_{0.5}$ spectrum at largest momentum transfer $Q=1.78$ Å^{-1} for $T=330$ K. The quasielastic broadening (1.43 μeV, HWHM) is well corresponding to the instrument energy range. Clearly, it is not related to the broadening observed with IN6 at the same temperature for a similar momentum transfer (Fig. 3). The broadening observed with IN6 appears in the IN16 spectrum under the form of an underlying flat background (Fig. 5 inset).

From these results it thus appears that the second inflection point shown by the curves of Fig. 2 at higher temperature corresponds to a motion having very different characteristics from those of a methyl rotation. In this framework, the simplest assumption one can make is to consider a ''jump'' of the whole CSA molecule in between two equilibrium positions and try to perform a fitting of the experimental scattering curves with such a model.

Under the assumption that the molecules perform instantaneous jumps, the rotational incoherent scattering function, for a single proton moving between two sites separated by a distance r can be written[12] as

$$S(\boldsymbol{Q},\omega)=A_0(\boldsymbol{Q})\,\delta(\omega)+A_1(\boldsymbol{Q})\,\frac{1}{\pi}\,\frac{\tau}{1+\omega^2\tau^2}. \qquad (23)$$

It can be noted that this model is exactly corresponding to that of a potential energy profile with two separated wells that is widely used for describing local diffusive motions in biological macromolecules.[32] τ is the correlation time (mean time between two jumps). The elastic $A_0(\boldsymbol{Q})$ and the quasielastic $A_1(\boldsymbol{Q})$ structure factors have the following expressions

$$A_0(\boldsymbol{Q})=\tfrac{1}{2}[1+j_0(\boldsymbol{Q}\cdot\boldsymbol{r})], \qquad (24)$$

$$A_1(\boldsymbol{Q})=\frac{1}{2}[1-j_0(\boldsymbol{Q}\cdot\boldsymbol{r})] \qquad (25)$$

in which $j_0(\boldsymbol{Q}\cdot\boldsymbol{r})$ is the Bessel spherical function of zero order.

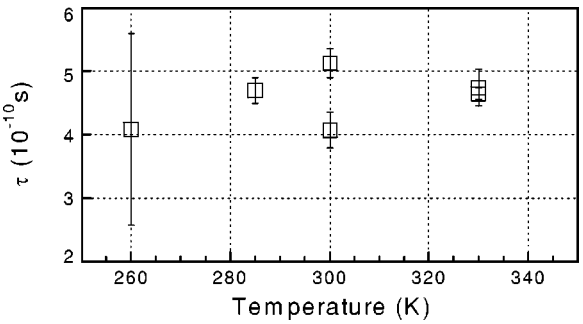

FIG. 13. Correlation time of the rigid body CSA motion as a function of the temperature.

Between 330 and 260 K good fits of the scattering curves were obtained. Calculated and experimental EISF are shown in Fig. 12 while the mean values of the correlation time as a function of the temperature are reported in Fig. 13 ($|\boldsymbol{r}|$ was kept constant at 1 Å). In this last figure the error bars are reflecting the spreading of the τ values as a function of $\boldsymbol{Q}$. As can be seen, already at 260 K it began to be difficult to extract the value of the quasielastic broadening since the scattering signal is more and more elastic. For this reason, at temperatures inferior or equal to 250 K, the experimental curves could not be fitted anymore. At this stage we might wonder if for this motion it would be also necessary to consider a distribution of the correlation times, especially if we note the significant increase of the EISF when the temperature is lowered (Fig. 12). Unfortunately, it is not possible to develop such an approach because of the limited amount of usable data. Considering such a fast decrease in the quasielastic intensity as a function of the temperature, we are led to assume that some transition is really happening around 250 K. In such a case, either the value of τ is changed in such a large proportion that it is exiting the time window seen by IN16 or the CSA motion is blocked at these temperatures. We carefully checked this point by our measurements carried out on IRIS at ISIS, which are reported in details elsewhere.[31] As IRIS has a 15 μeV energy resolution, we thought it should be possible to follow more precisely this dynamics at low temperatures. In fact on IRIS, in order to fit correctly our data at high temperatures, we needed to convolute the motion of methyls with the CSA motion. But, at temperatures lower than 250 K, it was enough to retain only the methyl dynamics as already found on IN6 at ILL for fitting these data. Only this procedure among numerous others we tried, allowed us first to fit correctly the data and also to recover quantitatively the same EISF that we found with IN6. These results strongly suggest that at temperatures inferior to 250 K the rigid-body CSA motion has disappeared, the molecules are blocked, likely inducing an extended static molecular disorder in the system. This is also precisely around this temperature that the distribution of the correlation times of the methyl motion becomes completely relevant.

V. CONCLUSION

The techniques of quasielastic neutron scattering have proved to be very powerful to give important information about the molecular dynamics in PANI/CSA system from the comparison that can be easily made in between the results obtained on a fully hydrogenated sample and a partially deuterated one.

All the results we found indicate that PANI/CSA has to be considered not really as a flexible polymer in a glassy state but as a disordered molecular solid in which the sublattice constituted by the intercalated counterions undergoes dynamical transitions. Indeed, in the whole explored energy range, the PANI chains appear as very stiff objects whose dynamics is likely mainly vibrational. If any diffusive components exist they have to be looked for inside a much longer time scale as previously measured by NMR.[33] From our point of view, the structural disorder is quite heterogeneous, not only because of the evident semicrystalline character of the films[6,29] but also by considering the evolution of the distribution of the correlation times of the methyl groups dynamics as a function of the temperature. We found that this distribution is probably arising from a combination of distributions of both activation energy and attempt frequency of the methyl's dynamics. At high temperatures (300–350 K) the structural heterogeneity is not emerging from dynamical measurements and the methyl groups appear as dynamically equivalent. The whole space available around each counterion is similarly explored for all of them. The whole population of CSA counterions might be considered as involved in an ergodic process for which all the available positional sites have the same probability to be occupied. When the temperature is lowered, this regime disappears to leave room to another one for which all the differences of molecular environments are progressively revealed. The slow motion of the CSA molecules is progressively frozen while intermolecular effects more and more influence the methyl groups. This evolution is somewhat reminiscent of that we may design as a ''glass transition'' of the counterion sublattice.

At this stage of the study, the next step is to know if this description applies first specifically for the conducting state of polyanilines and second for all kinds of counterions with which such an electrical regime can be obtained. The first element of answer to the first point we have is still a little bit ambiguous. When we perform inelastic measurements on a partially doped insulating sample on IRIS spectrometer, we did not recover the rigid body motion of the CSA. But that could be only due to the too small number of CSA ions present in this system resulting in a lack of scattered intensity. Another way to obtain an insulating sample containing still a large number of counterions is to perform a thermal aging of the sample.[34] We will publish elsewhere other results very recently obtained on a progressively aged sample, which show that the rigid body CSA motion is indeed related to the conducting state of the PANI/CSA.

In our opinion, all our results are contributing to describe the lattice dynamical states corresponding to the different regimes of electronic transport observed in PANI/CSA and can be qualitatively understood using the notion of localization length in a heterogeneous medium.[7] At high temperatures, the molecular dynamics clearly contributes to maintaining a localization length that is large enough to ensure a coherent transport of charge carriers through the whole

sample. When the temperature is decreased the system has a tendency to freeze in an extended static disordered state in which displacement of charge carriers is no more so globally favored. This effect is likely even stronger in the more disordered parts of the films separating nanocrystalline domains. The localization length turns shorter than the mean size of these connecting domains and that results in a semiconducting regime for the conductivity. Our work has the merit to show that in this process, the counterions play also a central role. For this reason, we have undertaken a large program of research for finding new counterions allowing improvement of both the electrical and mechanical performances of the films.[35] The details of all the involved microscopic mechanisms in this quite complex situation is still far from being completely elucidated but we hope that these results and others to come will help the theoretical models of transport in such systems to be further improved.

ACKNOWLEDGMENTS

We sincerely thank A.J. Dianoux and M. Gonzalez from ILL for their assistance.

*Corresponding author. FAX: (33)4-76-635-495. Email address: David.Djurado@ujf.grenoble.fr

†Permanent address: Institut Charles Sadron, 6, rue Boussingault, 67083 Strasbourg-Cedex, France.

[1] See, for example, M. D. McGehee, E. K. Miller, D. Moses, and A. J. Heeger, in *Advances in Synthetic Metals, Twenty Years of Progress in Science and Technology*, edited by P. Bernier, S. Lefrant, and G. Bidan (Elsevier, Amsterdam, 1999), p. 98.

[2] See, for example, A. G. MacDiarmid, and A. J. Epstein, in *Conjugated Polymeric Materials: Opportunities in Electronics, Optoelectronics and Molecular Electronics*, edited by J. L. Bredas and R. R. Chance (Kluwer Academic, Dordrecht, 1990), p. 53.

[3] Y. Cao, P. Smith, and A. J. Heeger, Synth. Met. **48**, 91 (1992); Y. Cao and A. J. Heeger, *ibid.* **52**, 193 (1992).

[4] A. G. Mac Diarmid and A. J. Epstein, Synth. Met. **69**, 85 (1995).

[5] M. Reghu, Y. Cao, D. Moses, and A. J. Heeger, Phys. Rev. B **47**, 1758 (1993).

[6] D. Djurado, Y. F. Nicolau, P. Rannou, W. Luzny, E. J. Samuelsen, P. Terech, M. Bée, and J. L. Sauvajol, Synth. Met. **101**, 764 (1999).

[7] R. S. Kohlman and A. J. Epstein, in *Handbook of Conducting Polymers*, 2nd ed, edited by T. A. Skotheim, R. L. Elsenbaumer, and J. R. Reynolds (Marcel-Dekker, New York, 1998), p. 85.

[8] M. Reghu, C. O. Yoon, D. Moses, and A. J. Heeger, in *Handbook of Conducting Polymers*, 2nd ed., edited by T. A. Skotheim, R. L. Elsenbaumer, and J. R. Reynolds (Marcel-Dekker, New York, 1998), p. 27.

[9] M. N. Bussac and L. Zuppiroli, Phys. Rev. B **47**, 5493 (1993).

[10] M. N. Bussac and L. Zuppiroli, Phys. Rev. B **49**, 5876 (1994).

[11] L. Zuppiroli, M. N. Bussac, S. Paschen, O. Chauvet, and L. Forro, Phys. Rev. B **50**, 5196 (1994).

[12] M. Bée, *Quasielastic Neutron Scattering, Principles and Applications in Solid State Chemistry, Biology and Materials Science* (Adam Hilger, New York, 1988).

[13] P. M. Beadle, Y. F. Nicolau, E. Banka, P. Rannou, and D. Djurado, Synth. Met. **95**, 29 (1998).

[14] G. Louarn, M. Lapkowski, S. Quillard, A. Pron, J. P. Buisson, and S. Lefrant, J. Phys. Chem. **100**, 6998 (1996).

[15] See all information on *http://www.ill.fr*

[16] B. Frick, A. Magerl, Y. Blanc, and R. Rebesco, Physica B **234–236**, 1177 (1990).

[17] A. P. Monkman, P. N. Adams, A. J. Milton, M. Scully, and S. J. Pomfret, Mol. Cryst. Liq. Cryst. Sci. Technol., Sect. A **236**, 189 (1993).

[18] L. Abell, S. J. Pomfret, P. N. Adams, and A. P. Monkman, Synth. Met. **84**, 127 (1997).

[19] R. E. Lechner, J. P. Amoureux, M. Bée, and R. Fouret, Commun. Phys. (London) **2**, 207 (1977).

[20] M. Bée, J. L. Sauvajol, and J. P. Amoureux, J. Phys. (Paris) **43**, 1797 (1982).

[21] M. Bée, J. Lajzérowicz-Bonneteau, and M. Le Bars-Combe, J. Chem. Phys. **97**, 7730 (1992).

[22] B. Frick and L. J. Fetters, Macromolecules **27**, 974 (1994).

[23] V. Arrighi, J. S. Higgins, A. N. Burgess, and W. S. Howells, Macromolecules **28**, 2745 (1995).

[24] V. Arrighi, J. S. Higgins, S. Mani, and L. Stoeber, Physica B **266**, 1 (1999).

[25] M. Bée, AGATHE, ILL Report ILL96BE11T, 1996 (unpublished).

[26] A. Chahid, A. Alegria, and J. Colmenero, Macromolecules **27**, 3282 (1994).

[27] V. Arrighi and J. S. Higgins, J. Chem. Soc., Faraday Trans. **93**, 1605 (1997).

[28] R. Mukhopadhyay, A. Alegria, J. Colmenero, and B. Frick, Macromolecules **31**, 3985 (1998).

[29] W. Luzny, E. J. Samuelsen, D. Djurado, and Y. F. Nicolau, Synth. Met. **90**, 19 (1997).

[30] J. E. Anderson and W. P. Slichter, J. Chem. Phys. **41**, 1922 (1964).

[31] M. Bée, D. Djurado, J. Combet, M. Telling, P. Rannou, A. Pron, and J. P. Travers, Physica B **301**, 49 (2001).

[32] W. Doster, S. Cusack, W. Petry, Nature (London) **337**, 754 (1989).

[33] S. Kaplan, E. M. Conwell, A. F. Richter, and A. G. MacDiarmid, Macromolecules **22**, 1669 (1989).

[34] P. Rannou, M. Nechtschein, J. P. Travers, D. Berner, A. Wolter, and D. Djurado, Synth. Met. **101**, 734 (1999).

[35] B. Dufour, P. Rannou, P. Fedorko, D. Djurado, J. P. Travers, and A. Pron, Chem. Mater. **13**, 4032 (2001).